Soft Matter

Accepted Manuscript

ROYAL SOCIETY OF CHEMISTRY

www.rsc.org/softmatter

Temperature Memory Effect in Amorphous Shape Memory Polymers

Kai Yu[1], H. Jerry Qi[1,*]

[1] The George Woodruff School of Mechanical Engineering, Georgia Institute of Technology, Atlanta, GA 30332, USA.

[*] Author to whom correspondence should be addressed: qih@me.gatech.edu

Abstract: A temperature memory effect (TME) refers to the ability of shape memory polymers (SMPs) to memorize the temperature at which pre-deformation was conducted. In the past few years, this TME was experimentally demonstrated by comparing the applied programming temperature (T_d) with a characteristic recovery temperature (T_c), which corresponds to either maximum recovery stress or free recovery speed. In these well designed experiments, T_c was observed to be close to T_d, which is consistent with the intuitively understanding of 'memorization'. However, since the polymer recovery behavior has been proved to be strongly dependent on various programming and recovery details, a new question that whether T_c is always equal to T_d in any thermo-temporal conditions remains to be addressed. In this paper, we answered this question by examining the free recovery profile of an acrylate based amorphous SMP. The recovery T_c, which is the temperature with maximum recovery speed versus recovery temperature, is shown to be strongly dependent on both programming and recovery conditions. Their detailed influence could be explained by using reduced time. During a thermomechanical working cycle of SMPs, in addition to the T_d, any other thermo-temporal conditions, such as holding time (t_h), cooling rate and recovery heating rate (q) etc., can affect the observed T_c by changing the reduced programming or recovery time. In this manner, the relation between T_c and T_d is not uniquely determined. Besides, the TME in SMPs can

only be achieved within a given temperature range. Both onset and offset of this temperature range is shown to be influenced by the programming history, but is independent on the recovery conditions.

Keywords: *Temperature memory effect; Multi-branched model; Shape memory polymers*

1. Introduction

The conventional definition of shape memory polymers (SMPs) is a class of stimuli-responsive smart materials that can be deformed at high temperature and subsequently be frozen upon cooling to fix the programmed temporary shape, which remains stable unless an environmental stimulus is applied, such as temperature [1-8], magnetic fields [9-14], light [15-20] and moisture [21, 22] etc. Depending on whether or not the external load still exists when the SMP is activated, the polymers demonstrate shape memory (SM) effect by providing recovery stresses or showing shape recovery, namely a constrained or free recovery process. Among the variety of external stimuli that might be utilized as the triggering mechanism, the most common one is direct heating to increase the temperature.

Although the basic concept of SMPs has been known for decades, recent advances have led to the discovery of previously uncovered memory properties that challenge our understanding of this type of polymer material [23-31]. For example, the programming condition has been shown to significantly affect the shape memory behavior of SMPs even if the same thermo-temporal recovery condition is used [27, 29, 30, 32-34]. A temperature memory effect (TME), in this occasion, refers to the capability of SMPs to memorize the applied programing temperatures (T_d). Early works in this area demonstrate that both of the free recovery curves and maximum recovery stress under strain constraint will be shifted to a higher recovery temperature if a higher programming temperature was used [4, 35]. Subsequently, Pierre et al. [28] tested the shape memory property in a polyvinyl alcohol (PVA) based nanocomposite, where the temperature memory is described such that the temperature corresponding to the maximum recovery stress is roughly identical to T_d. Xie et al [23, 25, 36] also reported the free recovery based TME

in Nafion polymer. The temperature at which a maximum shape recovery rate was observed was also shown to be close to the applied T_d. From these pioneer experimental investigations, one can gain recognition that the shape memory characteristic temperature (T_c), which is either corresponding to maximum recovery stress or shape recovery speed, can be quantitatively related to the programming temperature.

However, the question remains whether T_c would always be equal to T_d in any SM cycles, or their detailed relation is also dependent on other experimental parameters during the programming and recovery steps. Many previous works show that the free recovery curves of SMPs are strongly dependent on the packaging programming conditions, such as loading rate, holding time (t_h) and cooling rate etc [27, 30, 37-40]. Tobushi et al [41] also experimentally demonstrated the influence of recovery heating rate (q) on the free recovery behavior of SMPs. In case of higher q being applied, the amount of recovered strain is indeed lower when a given recovery temperature is reached, namely a delayed shape recovery. In this manner, T_c is also dependent on the recovery heating rate. More recently, Wang et al [42] also showed that free recovery based TME could only be observed within a specific range of recovery temperature, but not in its entire range of glass transition temperature (T_g). These observations indicate that the relation between T_c and T_d is not so straightforward as we expected. The detailed programming and recovery conditions during the SM cycle, as well as the polymer temperature dependent thermoviscoelastic properties, may determine T_c during the free recovery of SMPs, and should be considered when we study the TME.

In this paper, we study the TME of thermally responsive amorphous SMPs under the aforementioned considerations, and explore the detailed relation between T_c and T_d during

the polymer free shape recovery. Experimental observations firstly revealed the influence of programming temperature and heating rate on free shape recovery behavior of an acrylate based SMP material. A one dimensional (1D) multi-branch rheological model was then used to capture the experimental observations, and parametrically predicted the free recovery T_c under various programming and recovery conditions. We conclude that both the temperature range to observe TME in the SMPs, and the relation between T_c and T_d, are not unique. They are both dependent on the thermo-temporal history within a shape memory (SM) cycle. The TME in the SMPs is indeed a synergistic effect of both programming and recovery conditions on the material free recovery behavior.

2. Experiments

2.1 Material

The SMP material used in this study is an acrylate-based network polymer. Its liquid monomer tert-butyl acrylate (tBA), liquid cross-linker poly (ethylene glycol) dimethacrylate (PEGDMA) and the photo polymerization initiator (2, 2-dimethoxy-2-phenylacetophenone) in powder form are ordered from Sigma Aldrich (St. Louis, MO, USA) and used in their as received conditions without any further purification. The synthesis procedure of the SMP followed Yakacki et al [43] by mixing the tBA monomer, cross-linker and photo polymerization initiator with a weight ratio of 4000:1000:1, and the solution is then exposed in a UV irradiation for 10 min before the final heat treatment at 90°C for 1 hour to assist the complete conversion of monomers.

All the experiments involved in this paper were conducted on a Dynamic Mechanical Analyzer (DMA, TA Instruments, Model Q800, New Castle, DE, USA). The

SMP was cast into rectangular specimens with a uniform dimension of 10 mm×3 mm×0.2 mm.

2.2 DMA test

DMA tests were performed to characterize the glass transition behavior of the acrylate SMPs. The SMP specimen was firstly heated to 95 °C on the DMA machine and stabilized for 20 minutes to reach thermal equilibrium. During the experiment, the strain was oscillated at a frequency of 1 Hz with a peak-to-peak amplitude of 0.1% while the temperature was decreased from 95 °C to 5 °C at a rate of 1 °C/min.

2.3 Thermomechanical working cycle of SMPs

Free recovery tests of acrylate SMP were conducted on the DMA machine by using a strain controlled methods, and the detailed procedure follow the SM cycle shown in Figure 1a: In the programming step, the SMP is stretched to a target strain $e_{\max}$ (20%) with a constant loading rate $\dot{e}$ (0.01/s) at the programming temperature T_d, followed by a specified holding time (t_h) at T_d before being cooled to the shape fixing temperature T_L (20^{o}C) at a rate of 2.5°C/min. Once T_L is reached, the specimen is held for one hour then the tensile force is removed. In the free recovery step, the temperature is increased to the recovery temperature T_r at a given heating rate of q. The strain evolution during this step was used to calculate the time dependent shape recovery ratio.

Throughout the paper, the shape recovery ratio R_r and the shape recovery speed V_r are respectively defined as [25, 44]

$$R_r = 1 - e(t)/e_r \tag{1a}$$

and

$$V_r = \frac{\partial R_r}{\partial T_H}, \tag{1b}$$

where $e(t)$ is the strain evolution during the free recovery step, e_r is the strain measured at the start of the free recovery process, $T_H(t) = qt$ is the time dependent recovery temperature, and the characteristic recovery temperature T_c is taken to be the temperature corresponding to the maximum recovery speed (see Figure 1b).

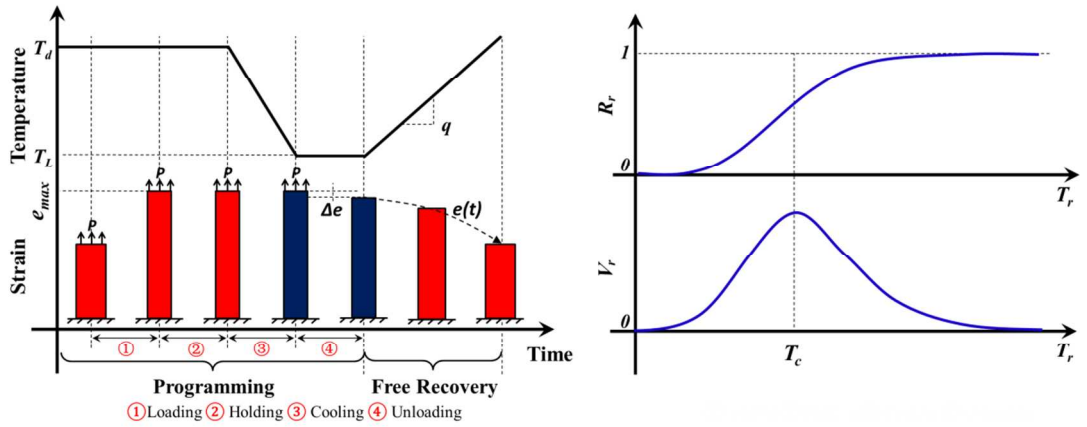

Figure 1. A schematic illustration of **(a)** the thermomechanical history of the programming and free recovery process in a SM cycle, and **(b)** the characteristic free recovery temperature T_c

3. Constitutive Modeling of SMPs

Currently, theoretical studies of shape memory phenomena in polymers are mainly based on two modeling approaches: phase evolution [45-50] and thermoviscoelastic modeling method [27, 51-55]. Here in this study, to capture the shape memory properties of the acrylate-based SMP, we use a multi-branched thermoviscoelastic constitutive model. The model resembles a generalized Maxwell element that consists of one equilibrium branch and several thermoviscoelastic nonequilibrium branches (number of n) to represent the multiple relaxation processes (for example, Rouse modes) of the polymer. E_{eq} and E_i is the elastic modulus in the equilibrium and nonequilibrium branches, respectively. $\tau_i(T)$ denotes the temperature dependent relaxation time in the dashpots. A

detailed description of the multi-branch model for SMP application can be found in Yu et al [27], which is also shown in the supplementary material of this paper. Its extension for 3D nonlinear model can be found in Westbrook et al [54] and Diani et al [53].

Here, it is assumed that the time-temperature shift for each branch follows the same rule. According to the well-established "thermorheological simplicity" principle [56] under a non-isothermal condition, the relaxation times (or viscosity) of each nonequilibrium branch vary as the temperature changes:

$$\tau_i = \alpha_T(T)\tau_i^0, \tag{2}$$

where $\alpha_T(T)$ is a time-temperature superposition (TTSP) shifting factor, and τ_i^0 is the reference relaxation time at the temperature when $\alpha_T(T)=1$.

Depending on whether the temperature is above or below a shifting temperature T_s [57], the shift factor $\alpha_T(T)$ is respectively calculated by the following two equations, namely the (Williams-Landel-Ferry) WLF equation [58] and the Arrhenius-Type equation [59]:

$$log\alpha_T(T) = -\frac{C_1\left(T-T_r\right)}{C_2+\left(T-T_r\right)}, \tag{3a}$$

$$ln\alpha_T(T) = -\frac{AF_c}{k_b}\left(\frac{1}{T}-\frac{1}{T_g}\right). \tag{3b}$$

where T_r is the WLF reference temperature, C_1 and C_2 are material constants that depend on the choice of T_r, A is a material constant, F_c is the configurational energy and k_b is Boltzmann's constant. T_s is taken to be the crossing point of two curves representing Eqs. 3a and 3b on a $\alpha_T(T)$ vs T plot.

The model parameters were determined by using the tan δ and storage modulus of the SMP obtained in the DMA tests. The identification procedure is briefly introduced in the supplementary material. A detailed model parameters identification method of the multi-branch model can be found in previous studies [27, 52, 53]. It should be noted that in this paper, the applied modeling method is based on linear thermoviscoelasticity. Cautions should be taken if a SMP demonstrates highly nonlinear or inelastic behavior. Small strain DMA test will be insufficient to characterize the thermoviscoelastic (or thermoviscoplastic) behaviors and thus may not be able to provide an accurate estimation of the SM performance. In this case, nonlinear modeling approach such as those presented by Abrahamson et al.[60], Tobushi et al.[61] and Srinivasa et al. [62] can be used.

As shown in Figure 2a, the identified parameters could enable the multi-branch model to successfully capture the experimental storage modulus and tanδ curves within the entire testing temperature range (5^{o} C-95^{o} C). The temperature dependent shift factors were then calculated by using Eq. 3 and plotted in Figure 2b as a function of temperature. The final set of model parameters are listed in Table 1. Compared with our previous work, where seven nonequilibrium branches are constructed in the multi-branch model, the amount of nonequilibrium branch in this study is extended to be sixteen with refined relaxation time distribution, which will enable a smooth and accurate prediction on the recovery speed curves versus recovery temperature.

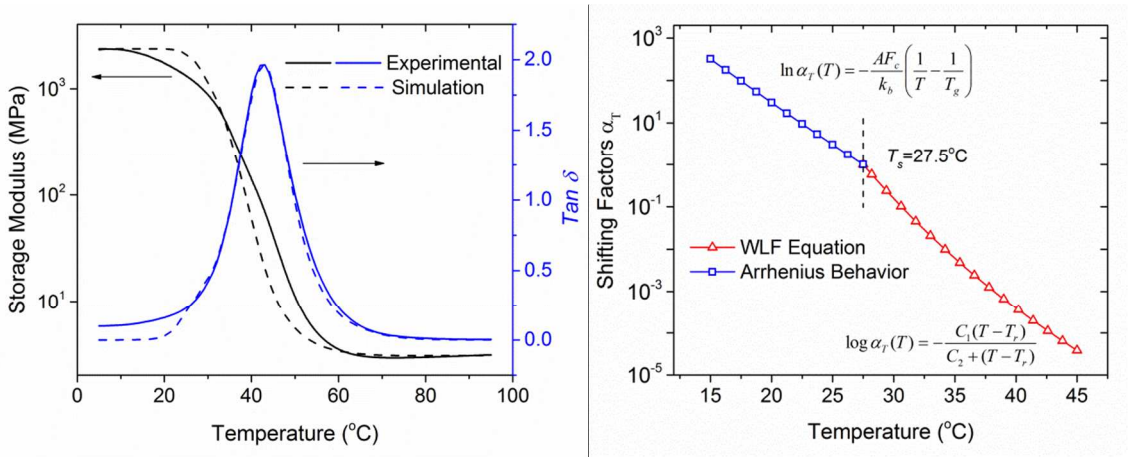

(a) **(b)**

Figure 2. (a) 1D estimation for the DMA result of SMP by using NLREG software. The original experimental curves are shown in solid lines. **(b)** Shifting factors at different temperatures: above 27.5 °C, shifting factors follow the WLF equation; below 27.5 °C, shifting factors follow the Arrhenius-Type behavior.

Table 1. Parameters of the multi-branched constitutive model

Parameters	***Values***	***Parameters***	***Values***
C_1	16.44	C_2	51.6 °C
$AF_c k_b^{-1}$	-40000 K	T_g	42.7 °C
T_s	27.5 °C	T_M	30 °C
E_{eq}	3.05 MPa		
E_i	(424.2, 424.2, 399.2, 276.6, 329.7, 245.3, 153.4, 64.4, 23.5, 7.51, 3.02, 1.50, 0.71, 0.43, 0.12, 0.16) MPa for $i \in [1,16]$		
τ_i^0	($10^{-0.5}$, 10^0, $10^{0.5}$, 10^1, $10^{1.5}$, 10^2, $10^{2.5}$, 10^3, $10^{3.5}$, 10^4, $10^{4.5}$, 10^5, $10^{5.5}$, 10^6, $10^{6.5}$, 10^7) s, for $i \in [1,16]$		

4. Results and Discussion

4.1 Experimental Observations

We start our discussions by firstly showing some experimental observations on the free recovery ratio and speed under different programming and recovery conditions. As a baseline SM cycle, the programming temperature T_d, the holding time t_h at T_d and the recovery heating rate q are respectively set to be 35°C, 60s and 1°C/min. Other

experimental setup is the same as that described in Section 2.3. As comparisons, another two SM cycles were performed: one with increased programming temperature (T_d=40 ^{o}C), while the other one with decreased heating rate (q=0.1 ^{o}C/min). The shape recovery ratio and speed in these three SM cycles are respectively plotted in Figure 3a and 3b as a function of recovery temperature (T_H).

As shown in Figure 3, both programing temperature and heating rate significantly affect the material free recovery profile: On one hand, increasing T_d from 35 ^{o}C to 40 ^{o}C will decrease the shape recovery speed under the same heating rate, and elevates the T_c from 34 ^{o}C to 38 ^{o}C. On the other hand, similar with previous study of Tobushi et al. [41], decreasing q increases the recovery speed versus recovery temperature, and consequently shift T_c to a small value. This is because a lower heating rate, which means longer heating time before reaching a given recovery temperature, would allow the SMPs to evolve more towards the equilibrium state and hence give a larger recovery strain. When the heating rate is set to be 0.1 ^{o}C/min, the T_c is seen to be decreased from 34 ^{o}C to 30 ^{o}C.

In addition to the experimental observations, simulation results based on the multi-branch model and predetermined model parameters are also plotted in Figure 3 as dash lines. It could be seen that the numerical simulations adequately capture the temperature dependent shape recovery ratio and normalized recovery speed. In the following, parametric studies based on the multi-branch model will be performed to investigate the influence of programing and recovery conditions on the TME in SMPs.

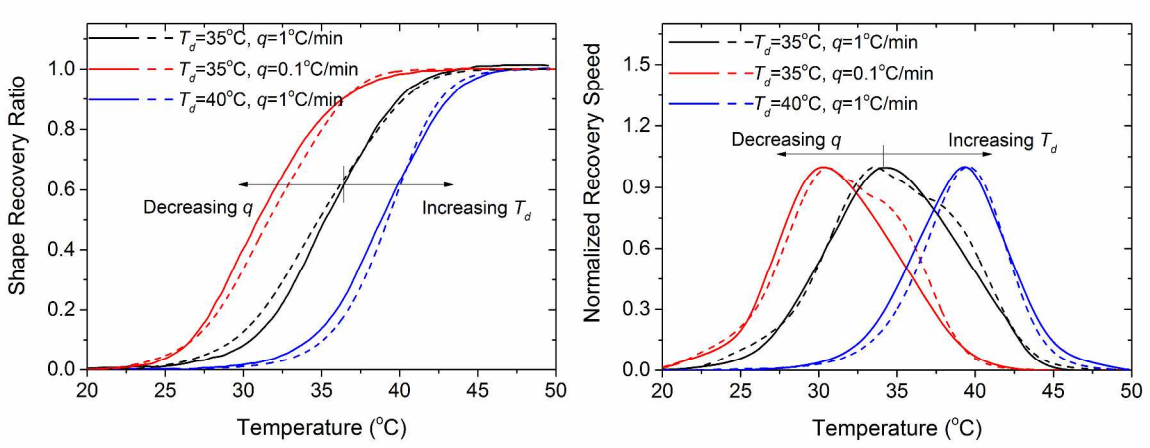

(a) **(b)**

Figure 3 Influence of programming temperature and heating rate on the temperature dependent. **(a)** shape recovery ratio and **(b)** normalized shape recovery speed. Note: the dash line denote simulation curves by using the 1D multi-branch model.

4.2 Influence of Programming Condition

The influence of T_d on the polymer free recovery profile is predicted and demonstrated in Figures 4a and 4b, where the T_d is gradually increased from 25 °C to 59 °C (2 °C of temperature interval) during the simulation. The holding time t_h at T_d and the heating rate during the free recovery are respectively set to be 60s and 1 °C/min in each case. Figure 4c further plots the T_c during the polymer free recovery as a function of applied T_d.

Two main features could be found from the numerical simulations in Figure 4. Firstly, within a specific temperature range (~30°C - ~47.5°C), increasing programming temperature will decrease the recovery speed versus recovery temperature. T_c increases with T_d in exhibiting a roughly linear relation. This obeys the recognition of traditional TME that T_c observed during the free recovery step is close to the T_d applied at programing step. Secondly, beyond this temperature range, changing T_d does not obviously affect the T_c. This prediction, that the TME could only be realized within a given temperature range, is consistent with the recent study of Wang et al [42].

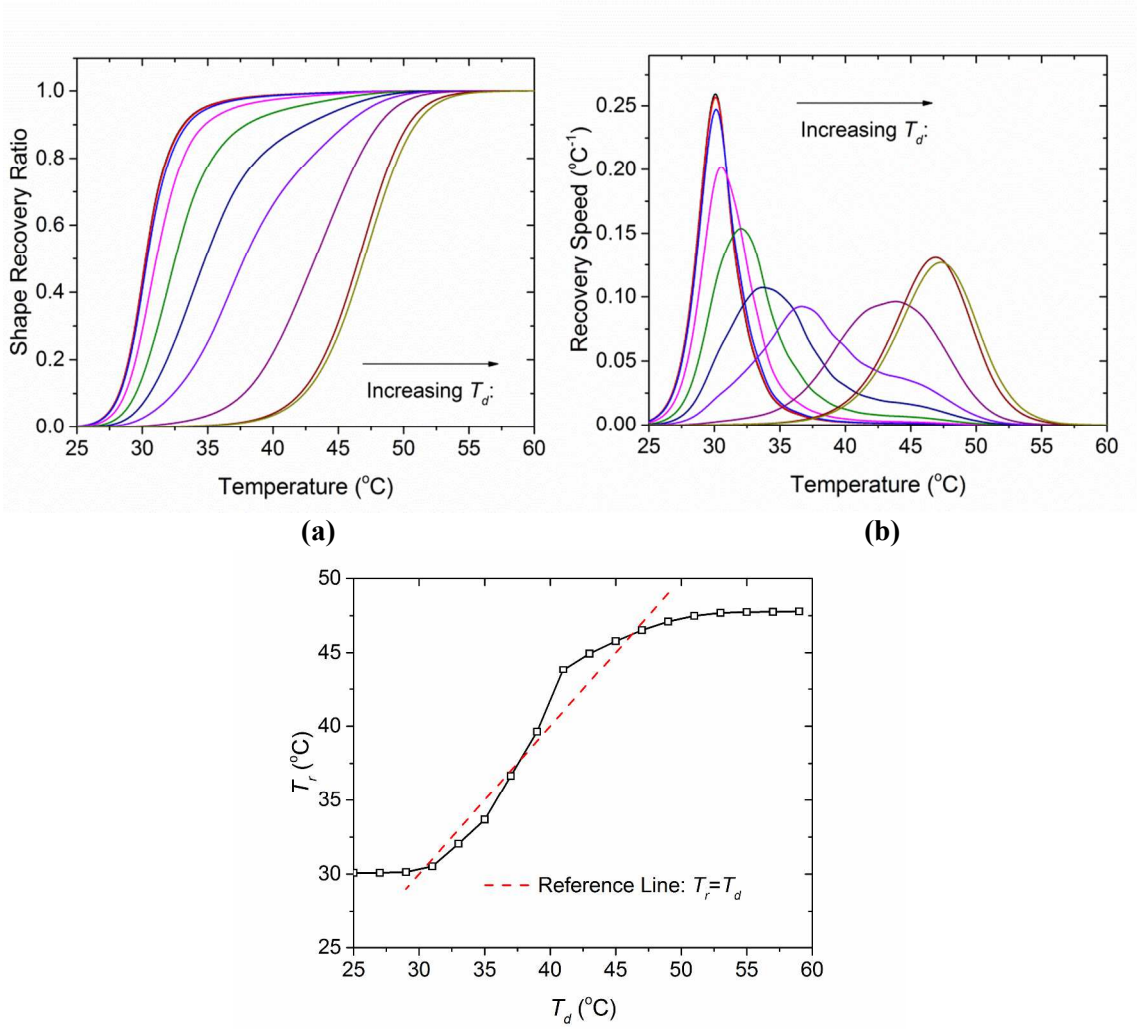

Figure 4. Parametric study on the influence of programing temperature. T_d increases from 25 °C to 59 °C with 2 °C of temperature interval. **(a)** Shape recovery ratio as a function of recovery temperature. **(b)** Shape recovery speed as a function of recovery temperature. **(c)** T_c as a function of T_d

The two features shown in Figure 4 could be explained by examining the stress distribution within each branch of the multi-branch model. Previously, we demonstrated that if the same thermo-temporal recovery conditions are applied on SMPs, their free recovery profiles are only dependent on the stress distribution after unloading, or namely the stress distribution at the beginning of recovery [27]. Figure 5a shows this stress distribution at the end of seven different programming conditions with different T_d (27.5 °C, 30 °C, 40 °C, 47.5 °C and 60 °C respectively).

As the temperature is higher than 47.5 ^{o}C, T_c is observed to be independent of T_d. This phenomenon can be explained as followings: when the SMPs are stretched at higher temperatures, the elastic strain development within each nonequilibrium branch is small due to the high mobility of dashpots. The stress relaxation in the subsequent holding and cooling steps will further release these nonequilibrium elastic strains. During the unloading at low temperature, removing the external load will cause a re-distribution of strains (due to the rebalance of forces to maintain overall equilibrium) in all the branches [24, 27], and internal stress state after unloading is that only the equilibrium spring remains in tension while the rest springs are being compressed (see Figure 5a for the case of T_d =47.5 ^{o}C and 60 ^{o}C). In this manner, when the temperature is raised again during the recovery step, only the equilibrium branch provides driven forces for viscous strain release (see Figure 5b) and material shape recovery, while the rest branches keep on resisting until the contained dashpots are activated. Since the nonequilibrium elastic stress are already released essentially before unloading for the case of T_d =47.5 ^{o}C, further increasing the programming temperature to 60 ^{o}C will not affect the rheological stress state, and therefore, the subsequent free recovery curve of SMPs are almost the same. This is the reason for T_d =47.5 ^{o}C being observed as the upper temperature limit for TME in the acrylate SMP as seen in Figure 4c.

However, when gradually decrease the programming temperature from 47.5 ^{o}C to 30 ^{o}C, the dashpots mobility is decreasing, and considerable elastic strain could be developed when stretching the multi-branch model, especially in branches with larger relaxation times. These elastic strains could not be totally released during the subsequent holding and cooling, and will be stable when the temperature is low. As seen in Figure 5a,

decreasing the programming temperature will change the rheological stress state after unloading in two ways: firstly, the stress magnitude in each nonequilibrium branch is increased. The intensified stress state will proportionally increase the releasing rate of viscous strain in the dashpots (see bottom figure in Figure 5b). Secondly, after the stress re-distribution among all the branches during the unloading, more and more nonequilibrium springs will remain stretched in addition to the equilibrium spring. These branches will provide additional driven forces for the shape recovery of the multi-branch model, and consequently increase the recovery speed.

In the rheological multi-branch model, this additional driven force, namely the tensile stresses in the nonequilibrium branches at the beginning of recovery, is essentially representing the internal energy stored in the real polymer system after the programing step. When stretching the polymer network at lower temperatures, mobility of polymer chains might be insufficient for them to adjust the self-conformation and fully comply with the external deformation. In this manner, in addition to the network entropy change, some internal energy will also be generated and stored within the SMPs. This internal energy is originated from the alteration in macromolecule bond length and angle during the deformation, and will assist the spontaneous shape recovery of the polymer network upon reheating.

According to the influence of programming temperature as revealed in Figure 5a, it seems that decreasing the programming temperature is a good choice to increase the shape recovery speed. But this will sacrifice the material's shape fixing ability because the material tends to be unstable during unloading and a large portion of the programmed deformation is recovered right after unloading [27], which is unfavorable in most

engineering applications. For example, when T_d =30 °C, only ~41% of the programmed strain is fixed after unloading. Further decrease the programming temperature will continually decrease the polymer's shape fixity, but does affect the stress state too much. In this manner, the recovery T_c will remain unchanged when T_d is below 30 °C.

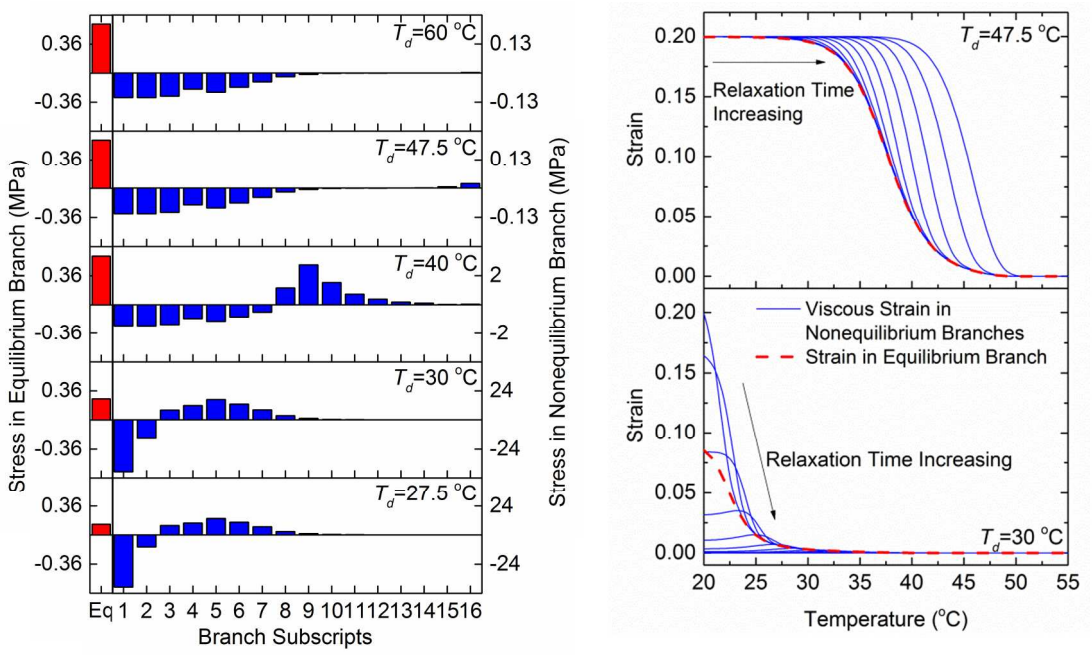

(a) **(b)**

Figure 5. (a) Stress distribution after unloading in seven different programing conditions. **(b)** Viscous strain release in each nonequilibrium branch and strain evolution in the equilibrium branch for the case of T_d=47.5 °C and T_d=30 °C

Now it is clear that the rheological stress state at the beginning of free recovery is the key to determine T_c. Previously, we have demonstrated that this stress state is only dependent on the reduced programming time t_r [27]. For non-isothermal process,

$$t_r = \int_0^t \frac{ds}{\alpha(T)}, \tag{6}$$

where t is the physical time and T is the temperature evolution during the programming step. Therefore, in addition to T_d, any other thermo-temporal programming conditions, such as holding time t_h after loading, cooling rates, and shape fixing temperature T_L etc.,

can also affect the recovery speed and the T_c by changing the reduced programming time and then consequently the rheological stress state. Here, we select the t_h as the parametric variable, and the predicted free recovery curves are shown in Figure 6a. The T_d and heating rate q are set to be 35 ^{o}C and 1 ^{o}C/min respectively in each simulation case.

As shown in the figure, increasing the holding time t_h will decrease the recovery speed because it plays the same role as increasing T_d in determining the reduced programming time. Besides, two boundary holding times are revealed from the figure: one represents the extreme condition that no holding time is applied (black curve). While for the second one, it indicates a 6×10^4s (~17 hours) holding time at T_d =35 ^{o}C is long enough to essentially release the elastic stresses in nonequilibrium branches during the programming, and the corresponding recovery profile is therefore the same as that with t_h =6×10^8 s (~19 years) .

Subsequently, Figure 6b summarizes the recovery T_c as a function of both T_d and holding time t_h. Clearly, the relation between T_c and T_d is not unique under the influence of t_h. A longer holding time will increase the T_c towards a saturated level at ~ 47.5 ^{o}C. Besides, both onset and offset value of the temperature range with TME observed decreases with the holding time increment.

For the curves in Figure 6b, after shifting each of them horizontally to a reference holding time t_{h0}, namely by

$$T_c(T_d, t_h) = T_c(\alpha_{th} T_d, t_{h0}), \tag{7a}$$

where α_{th} is the holding time dependent shift factors, a master curve can be constructed as shown in Figure 6c. The corresponding shift factors are plotted in Figure 6d as a

function of holding time. A linear relation between α_{th} and t_h is then revealed in the semi-log scale. By using the nonlinear regression method, we approximate the relation as

$$\alpha_{th} = 0.85 + 0.083 \log(\frac{t_h}{t_{h0}}). \quad (7b)$$

Within the temperature range with clear TME observed, Eq. 7 quantitatively demonstrates the packaging effect of both programming temperature and holding time on the T_c. That is, when a large holding time is applied during the programming step, the corresponding shift factor will be exponentially ramped and therefore a smaller T_d should be used if an equivalent T_c is expected. Otherwise the T_c will be monotonically increased. The analysis on the effect of increasing T_d and t_h can be extended to the influence of other thermo-temporal programming conditions, such as decreasing loading rate, cooling rates, or increase the stabilization time at T_L etc.

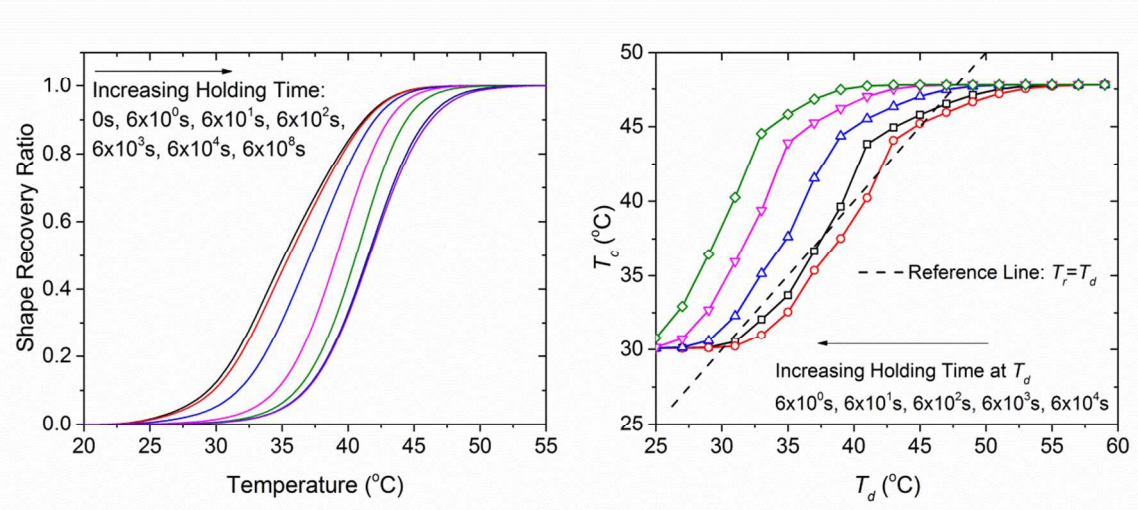

(a) **(b)**

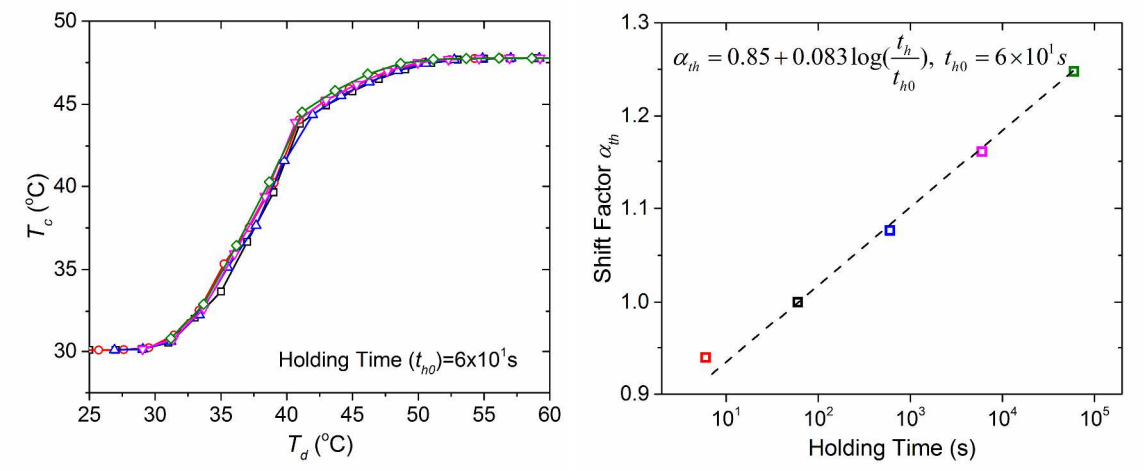

(c) **(d)**

Figure 6. Influence of both T_d and holding time on the free recovery profiles and T_c of SMPs. **(a)** The predicted free recovery curves with different holding times. T_d=35 °C. **(b)** T_c plotted as a function of both holding time and T_d. **(c)** The constructed master curve of T_c. the reference holding time t_{h0}=6×10^{1}s. **(d)** The holding time dependent shift factors during the construction of master curve.

4.3 Influence of Recovery Conditions

In addition to the programming condition, we will show in this section that the relation between T_c and T_d is also dependent on the free recovery condition. Considering the SM cycle shown in Figure 1a, the only parametric variable under investigation is the recovery heating rate q. Figure 7a shows the predicted free recovery curves with q increasing from 10^{-3} °C/min to 10^2 °C/min. All the programming procedures are set to be identical in each simulation case with T_d= 35 °C and holding time equal to 60s.

As demonstrated in our previous study [27], if the SMPs are experienced by the same programming step, their free recovery ratio is only dependent on the reduced recovery time, and a larger reduced recovery time will lead to a higher recovery ratio, namely:

$$R_r = R_r(t_r) \tag{8a}$$

with

$$t_r = \int_{T_L}^{T_H} \frac{dT}{q\alpha(T)}\ , \tag{8b}$$

where T_H is a given recovery temperature. Eq. 8b indicates that a larger heating rate will decrease the reduced recovery time and then consequently the recovery ratio when T_H is reached, as confirmed in Figure 7a. Figure 7b summarizes the recovery T_c as a function of both T_d and q. In addition to the revealed relation between T_c and T_d that is dependent on q, the temperature range to observe TME is shown to be unchanged upon changing the heating rate.

Subsequently, by shifting each curves in Figure 7b vertically into to a reference heating rate (q_0=10^0 °C/min) according to

$$T_c(T_d, q) = \frac{1}{\alpha_q} T_c(T_d, q_0) \tag{9a}$$

where α_q is a heating rate dependent shift factor, the curves are seen to be rejoined together to form a master curve, as shown in Figure 7c. The corresponding shift factors are summarized in Figure 7d. In the semi-log scale, the shift factor is linearly decreased as the increment of heating rate, namely:

$$\alpha_q = 1 - 0.092 \log(\frac{q}{q_0}) \tag{9b}$$

Eq. 9 quantitatively approximates the influence of recovery heating rate on the T_c with two features revealed: firstly, when a larger heating rate q is applied during the polymer free recovery step, both the shift factor and corresponding T_c will be decreased. Secondly, different from the above mentioned effect of programing condition, there is no boundary heating rate condition for the influence of heating rate. Keeping on increasing q will continually elevate T_c towards the target T_H. An infinitely large value is representing an isothermal recovery condition, where the T_c is always equal to T_H regardless of the applied programming temperature. In the opposite, if no heat is applied during the

recovery step, namely q=0, a thermally simple SMP can still recover into the original shape, even though this process may take for several years [8, 27]. Under this condition, T_c is equal to the shape fixing temperature T_L.

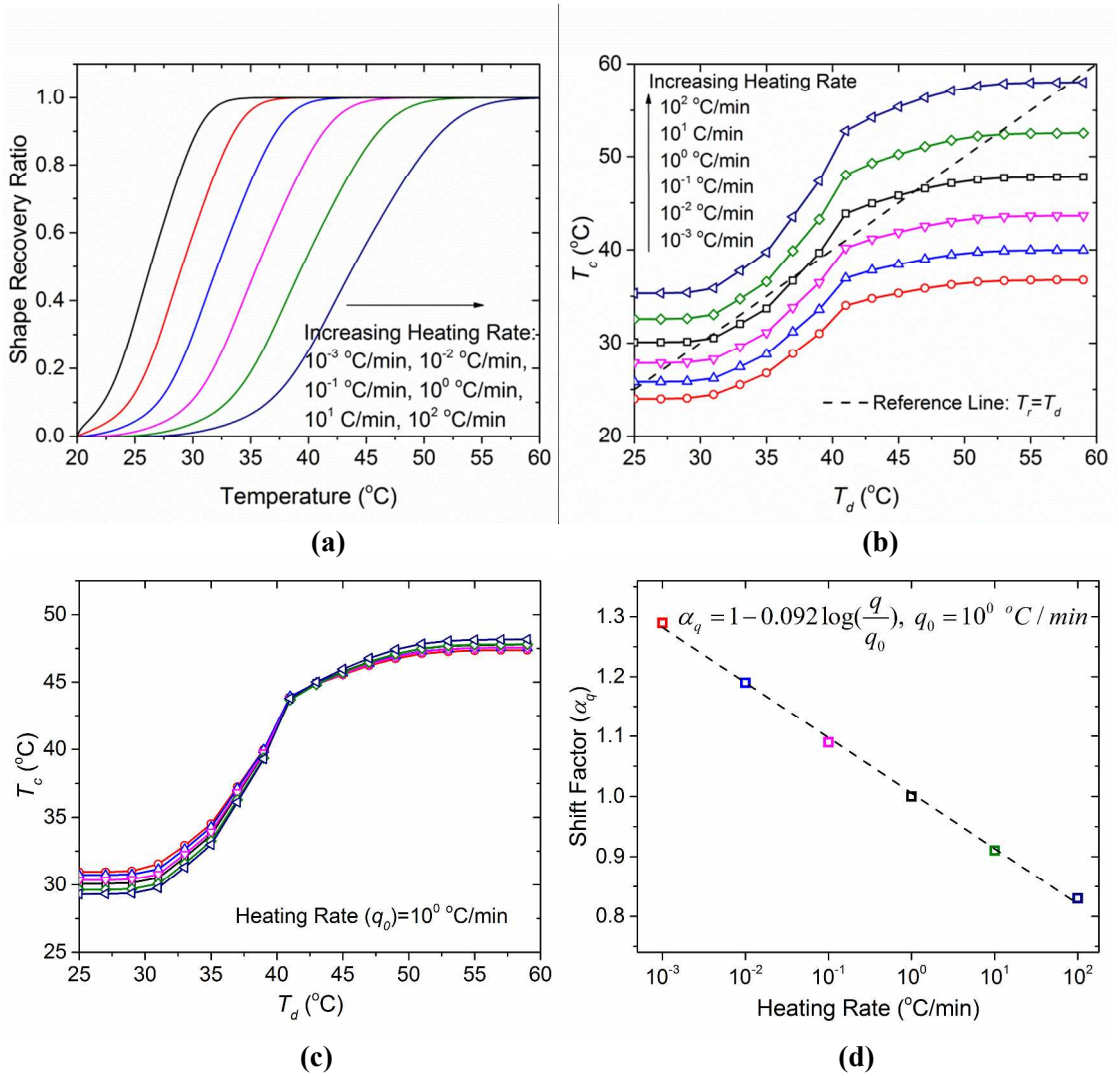

Figure 7. Influence of both T_d and heating rate q on the free recovery profiles and T_c of SMPs. **(a)** The predicted free recovery curves with different heating rates. T_d=35 °C and holding time equals to 6s. **(b)** T_c plotted as a function of both T_d and q. **(c)** The constructed master curve of T_c. The reference heating rate q_0=10^0 °C/min. **(d)** The heating rate dependent shift factors during the construction of master curve.

5. Conclusion

In this paper, from both experimental and theoretical point of view, we investigated the temperature memory effect (TME) in the acrylate based amorphous shape memory polymer (SMP). Different from the tradition definition of TME in the SMPs, our study indicates that the characteristic recovery temperature (T_c), which is the temperature with maximum recovery speed, is not always equal to the programming temperature (T_d). By revealing the underlying mechanism, we can gain a deeper understanding of how the programming and recovery conditions will affect the free recovery behavior of SMPs synergistically, which consequently provides a facile strategy to optimize the shape memory performance of SMPs by adjusting their thermomechanical working conditions, instead of developing new polymer systems. Such strategy offers huge convenience for engineering SMPs in the industry, especially in the field of medical, aeronautics and astronautics, where a long period of performance verification and official approval is typically expected.

Reference

1. Lendlein, A. and S. Kelch, *Shape-memory polymers.* Angew Chem Int Ed Engl, 2002. **41**(12): p. 2035-57.
2. Liu, C., H. Qin, and P.T. Mather, *Review of progress in shape-memory polymers.* Journal of Materials Chemistry, 2007. **17**(16): p. 1543-1558.
3. Chung, T., A. Rorno-Uribe, and P.T. Mather, *Two-way reversible shape memory in a semicrystalline network.* Macromolecules, 2008. **41**(1): p. 184-192.
4. Gall, K., et al., *Thermomechanics of the shape memory effect in polymers for biomedical applications.* Journal of Biomedical Materials Research Part A, 2005. **73A**(3): p. 339-348.
5. Mather, P.T., X.F. Luo, and I.A. Rousseau, *Shape Memory Polymer Research.* Annual Review of Materials Research, 2009. **39**: p. 445-471.
6. Yu, K., et al., *Carbon nanotube chains in a shape memory polymer/carbon black composite: To significantly reduce the electrical resistivity.* Applied Physics Letters, 2011. **98**(7).
7. Yu, K., Y.J. Liu, and J.S. Leng, *Conductive Shape Memory Polymer Composite Incorporated with Hybrid Fillers: Electrical, Mechanical, and Shape Memory Properties.* Journal of Intelligent Material Systems and Structures, 2011. **22**(4): p. 369-379.

8. Ge, Q., et al., *Prediction of temperature-dependent free recovery behaviors of amorphous shape memory polymers.* Soft Matter, 2012. **8**(43): p. 11098-11105.
9. Mohr, R., et al., *Initiation of shape-memory effect by inductive heating of magnetic nanoparticles in thermoplastic polymers.* Proceedings of the National Academy of Sciences of the United States of America, 2006. **103**(10): p. 3540-3545.
10. Buckley, P.R., et al., *Inductively heated shape memory polymer for the magnetic actuation of medical devices.* Ieee Transactions on Biomedical Engineering, 2006. **53**(10): p. 2075-2083.
11. Schmidt, A.M., *Electromagnetic activation of shape memory polymer networks containing magnetic nanoparticles.* Macromolecular Rapid Communications, 2006. **27**(14): p. 1168-1172.
12. He, Z.W., et al., *Remote Controlled Multishape Polymer Nanocomposites with Selective Radiofrequency Actuations.* Advanced Materials, 2011. **23**(28): p. 3192-3196.
13. Kumar, U.N., et al., *Non-contact actuation of triple-shape effect in multiphase polymer network nanocomposites in alternating magnetic field.* Journal of Materials Chemistry, 2010. **20**(17): p. 3404-3415.
14. Yu, K., et al., *Design considerations for shape memory polymer composites with magnetic particles.* Journal of Composite Materials, 2013. **47**(1): p. 51-63.
15. Jiang, H.Y., S. Kelch, and A. Lendlein, *Polymers move in response to light.* Advanced Materials, 2006. **18**(11): p. 1471-1475.
16. Koerner, H., et al., *Remotely actuated polymer nanocomposites - stress-recovery of carbon-nanotube-filled thermoplastic elastomers.* Nature Materials, 2004. **3**(2): p. 115-120.
17. Lendlein, A., et al., *Light-induced shape-memory polymers.* Nature, 2005. **434**(7035): p. 879-882.
18. Li, M.H., et al., *Light-driven side-on nematic elastomer actuators.* Advanced Materials, 2003. **15**(7-8): p. 569-572.
19. Scott, T.F., R.B. Draughon, and C.N. Bowman, *Actuation in crosslinked polymers via photoinduced stress relaxation.* Advanced Materials, 2006. **18**(16): p. 2128-+.
20. Scott, T.F., et al., *Photoinduced plasticity in cross-linked polymers.* Science, 2005. **308**(5728): p. 1615-1617.
21. Huang, W.M., et al., *Water-driven programmable polyurethane shape memory polymer: Demonstration and mechanism.* Applied Physics Letters, 2005. **86**(11): p. -.
22. Jung, Y.C., H.H. So, and J.W. Cho, *Water-responsive shape memory polyurethane block copolymer modified with polyhedral oligomeric silsesquioxane.* Journal of Macromolecular Science Part B-Physics, 2006. **45**(4): p. 453-461.
23. Xie, T., *Tunable polymer multi-shape memory effect.* Nature, 2010. **464**(7286): p. 267-270.
24. Yu, K., et al., *Mechanisms of multi-shape memory effects and associated energy release in shape memory polymers.* Soft Matter, 2012. **8**(20): p. 5687-5695.

25. Xie, T., K.A. Page, and S.A. Eastman, *Strain-Based Temperature Memory Effect for Nafion and Its Molecular Origins.* Advanced Functional Materials, 2011. **21**(11): p. 2057-2066.
26. Xie, T., X.C. Xiao, and Y.T. Cheng, *Revealing Triple-Shape Memory Effect by Polymer Bilayers.* Macromolecular Rapid Communications, 2009. **30**(21): p. 1823-1827.
27. Yu, K., G. Qi, and H.J. Qi, *Reduced time as a unified parameter determining fixity and free recovery of shape memory polymers.* Nature communications, 2014. **5**: p. 3066.
28. Miaudet, P., et al., *Shape and temperature memory of nanocomposites with broadened glass transition.* Science, 2007. **318**(5854): p. 1294-1296.
29. Chen, X. and T.D. Nguyen, *Influence of thermoviscoelastic properties and loading conditions on the recovery performance of shape memory polymers.* Mechanics of Materials, 2011. **43**: p. 127-138.
30. Castro, F., et al., *Time and Temperature Dependent Recovery of Epoxy-Based Shape Memory Polymers.* Journal of Engineering Materials and Technology-Transactions of the Asme, 2011. **133**(2).
31. Sun, L. and W.M. Huang, *Mechanisms of the multi-shape memory effect and temperature memory effect in shape memory polymers.* Soft Matter, 2010. **6**(18): p. 4403-4406.
32. Hu, J.L., F.L. Ji, and Y.W. Wong, *Dependency of the shape memory properties of a polyurethane upon thermomechanical cyclic conditions.* Polymer International, 2005. **54**(3): p. 600-605.
33. Cui, J., K. Kratz, and A. Lendlein, *Adjusting shape-memory properties of amorphous polyether urethanes and radio-opaque composites thereof by variation of physical parameters during programming.* Smart Materials & Structures, 2010. **19**(6).
34. Bothe, M., F. Emmerling, and T. Pretsch, *Poly(ester urethane) with Varying Polyester Chain Length: Polymorphism and Shape-Memory Behavior.* Macromolecular Chemistry and Physics, 2013. **214**(23): p. 2683-2693.
35. Miyamoto, Y., et al., *Memory effect on the glass transition in vulcanized rubber.* Physical Review Letters, 2002. **88**(22).
36. Li, J.J. and T. Xie, *Significant Impact of Thermo-Mechanical Conditions on Polymer Triple-Shape Memory Effect.* Macromolecules, 2011. **44**(1): p. 175-180.
37. Chen, X. and T.D. Nguyen, *Influence of thermoviscoelastic properties and loading conditions on the recovery performance of shape memory polymers.* Mechanics of Materials, 2011. **43**(3): p. 127-138.
38. J.W., A., Gyaneshwar P. T·, and J.W. B., *Strain rate- and temperature-dependent tensile properties of an epoxy-based, thermosetting, shape memory polymer (Veriflex-E).* Mech Time-Depend Mater, 2011. **16**(2): p. 205-221.
39. McClung, A., G. Tandon, and J. Baur, *Deformation rate-, hold time-, and cycle-dependent shape-memory performance of Veriflex-E resin.* Mechanics of Time-Dependent Materials: p. 1-14.
40. McClung, A.J.W. and M.B. Ruggles-Wrenn, *Strain Rate Dependence and Short-Term Relaxation Behavior of a Thermoset Polymer at Elevated Temperature:*

Experiment and Modeling. Journal of Pressure Vessel Technology-Transactions of the Asme, 2009. **131**(3).
41. Tobushi, H., et al., *Thermomechanical constitutive model of shape memory polymer.* Mechanics of Materials, 2001. **33**(10): p. 545-554.
42. Wang, Y.R., et al., *Relation between temperature memory effect and multiple-shape memory behaviors based on polymer networks.* Rsc Advances, 2014. **4**(39): p. 20364-20370.
43. Yakacki, C.M., et al., *Unconstrained recovery characterization of shape-memory polymer networks for cardiovascular applications.* Biomaterials, 2007. **28**(14): p. 2255-2263.
44. Lendlein, A. and R. Langer, *Biodegradable, elastic shape-memory polymers for potential biomedical applications.* Science, 2002. **296**(5573): p. 1673-1676.
45. Liu, Y.P., et al., *Thermomechanics of shape memory polymers: Uniaxial experiments and constitutive modeling.* International Journal of Plasticity, 2006. **22**(2): p. 279-313.
46. Muller, W.W. and T. Pretsch, *Hydrolytic aging of crystallizable shape memory poly(ester urethane): Effects on the thermo-mechanical properties and visco-elastic modeling.* European Polymer Journal, 2010. **46**(8): p. 1745-1758.
47. Kafka, V., *Shape memory polymers: A mesoscale model of the internal mechanism leading to the SM phenomena.* International Journal of Plasticity, 2008. **24**(9): p. 1533-1548.
48. Chen, Y.C. and D.C. Lagoudas, *A constitutive theory for shape memory polymers. Part I-Large deformations.* Journal of the Mechanics and Physics of Solids, 2008. **56**(5): p. 1752-1765.
49. Long, K.N., M.L. Dunn, and H.J. Qi, *Mechanics of soft active materials with phase evolution.* International Journal of Plasticity, 2010. **26**(4): p. 603-616.
50. Qi, H.J., et al., *Finite deformation thermo-mechanical behavior of thermally induced shape memory polymers.* Journal of the Mechanics and Physics of Solids, 2008. **56**(5): p. 1730-1751.
51. Lin, J.R. and L.W. Chen, *Shape-memorized crosslinked ester-type polyurethane and its mechanical viscoelastic model.* Journal of Applied Polymer Science, 1999. **73**(7): p. 1305-1319.
52. Yu, K., et al., *A thermomechanical constitutive model for an epoxy based shape memory polymer and its parameter identifications.* Mechanics of Time-Dependent Materials, 2014. **18**(2): p. 453-474.
53. Diani, J., et al., *Predicting thermal shape memory of crosslinked polymer networks from linear viscoelasticity* International Journal of Solids and Structure, 2012. **49**(5): p. 793-799.
54. Westbrook, K.K., et al., *A 3D Finite Deformation Constitutive Model for Amorphous Shape Memory Polymers: A Multi-Branch Modeling Approach for Nonequilibrium Relaxation Processes,.* Mechanics of Materials, 2011. **43**(12): p. 853-869.
55. Nguyen, T.D., et al., *A thermoviscoelastic model for amorphous shape memory polymers: Incorporating structural and stress relaxation* Journal of the Mechanics and Physics of Solids, 2008. **56** (9): p. 2792-2814

56. Rubinstein, M. and R.H. Colby, *Polymer physics*. 2003, New York: Oxford University Press, Oxford.
57. O'Connell, P.A. and G.B. McKenna, *Arrhenius-type temperature dependence of the segmental relaxation below T-g.* Journal of Chemical Physics, 1999. **110**(22): p. 11054-11060.
58. Williams, M.L., R.F. Landel, and J.D. Ferry, *Temperature Dependence of Relaxation Mechanisms in Amorphous Polymers and Other Glass-Forming Liquids.* Physical Review, 1955. **98**(5): p. 1549-1549.
59. Di Marzio, E.A. and A.J.M. Yang, *Configurational entropy approach to the kinetics of glasses.* Journal of Research of the National Institute of Standards and Technology, 1997. **102**(2): p. 135-157.
60. Abrahamson, E.R., et al., *Shape memory mechanics of an elastic memory composite resin.* Journal of Intelligent Material Systems and Structures, 2003. **14**(10): p. 623-632.
61. Tobushi, H., et al., *Thermomechanical constitutive modeling in shape memory polymer of polyurethane series.* Journal of Intelligent Material Systems and Structures, 1997. **8**(8): p. 711-718.
62. Ghosh, P. and A.R. Srinivasa, *A Two-network thermomechanical model of a shape memory polymer.* International Journal of Engineering Science, 2011. **49**(9): p. 823-838.